

Localization and Quantum State Transfer in Coupled Cavity Arrays

A. Broman, M. Radulaski, and R. Scalettar
Physics Department, University of California Davis

Coupled cavity arrays (CCAs), in which photons interact with atom-like emitters, have recently received significant attention for their applicability to quantum many-body simulations and quantum information processing. We investigate the use of emitters to induce localization and facilitate quantum state transfer (QST) in CCAs operating under the Tavis-Cummings-Hubbard model. These questions are probed with a computational model using exact diagonalization. We find that the introduction of an emitter to an emitter-free CCA produces localized modes with eigenvalues outside of the band. Secondly, we demonstrate the similarities between a CCA with an emitter in each outermost cavity and a CCA with modified outermost intercavity couplings, the latter of which has been shown to facilitate high-fidelity QST. This second result suggests that for QST applications, the introduction of emitters to a CCA could serve as an alternative to adjusting the intercavity couplings.

I. INTRODUCTION

Strong interactions between light and matter can be induced by trapping photons and atom-like emitters within an optical cavity. The study of such systems constitutes the field of cavity quantum electrodynamics (QED). Over the past two decades, the experimental realization of such cavity systems has allowed for the study of quantum many-body phenomena, including the simulation of phenomena encountered in condensed matter physics [1]. In contrast to condensed matter systems, which typically contain on the order of 10^{23} particles, cavity QED systems permit the manipulation of individual system components. This level of experimental control makes them attractive candidates for performing simulations of quantum many-body phenomena. In addition, cavity QED systems have applications in quantum information processing, where they have been proposed as a potential implementation of spin chains for quantum state transfer [2–4]. Finally, cavity systems permit the emergence of polaritons, or quasiparticles consisting of a superposition of photonic and atomic excitations [1, 2, 5]. The study of polaritons may allow us to probe new strongly correlated regimes of light-matter interaction.

In recent years, a type of cavity system known as a coupled cavity array (CCA) has received a considerable amount of attention [1, 6, 7]. A CCA consists of a chain of optical cavities, each of which may contain one or more atom-like emitters coupled to the cavity's electromagnetic field. Photons may hop between adjacent cavities in the CCA due to the overlap of neighboring resonance modes.

CCAs have become increasingly experimentally viable in recent years [8, 9]. In order to observe quantum many-body phenomena, the system must exist in the strong coupling regime of cavity quantum electrodynamics, where light-matter interactions are stronger than losses to the environment. Modern optical cavities achieve this by localizing light on the nanometer scale. One of the commonly used optical resonators for these studies is the photonic crystal cavity, formed by periodic refractive index alteration at the sub-wavelength scale. Although the cavity is a few micrometers across, nanoholes fabricated in the material change the index of refraction such that light is localized to an area of a few hundred nanometers [8].

One of the attractive choices for quasi-atoms in solid-state

systems are color centers formed as lattice defects in semiconductors [10]. The defect causes electron wavefunctions to localize at that point, which creates an isolated set of energy levels within a solid-state material. The most common material substrates for this purpose are silicon carbide and diamond. For example, [11] describes a photonic crystal cavity with a triangular cross-section, fabricated in a silicon carbide substrate with various possible color centers.

II. TAVIS-CUMMINGS-HUBBARD MODEL WITH EXACT DIAGONALIZATION

Our research focuses on the theoretical study of CCAs operating under the Tavis-Cummings-Hubbard model. This model describes an array of coupled cavities in which each cavity may contain one or more two-level emitters. The number of cavities is given by N . A total of M excitations is present in the system. At any given time, each excitation may exist as a photon or as an emitter in the excited state.

We study these CCA systems using exact diagonalization. The advantage of this approach is that we obtain exact values for the eigenenergies of the system. This precision, however, means that memory and runtime constraints limit us to studying small arrays. Modeling and diagonalization were implemented in Python 3 using standard packages such as NumPy, with no specialized software being required.

The Tavis-Cummings-Hubbard Hamiltonian is given by:

$$H = -J \sum_n (a_{n+1}^\dagger a_n + a_n^\dagger a_{n+1}) + \sum_n [\omega_c a_n^\dagger a_n + \sum_e (\omega_e \sigma_n^+ \sigma_n^- + g(\sigma_n^+ a_n + a_n^\dagger \sigma_n^-))] \quad (1)$$

Here, J is the rate of photon hopping between cavities and g is the rate of cavity-emitter photon exchange. The cavity frequency is given by ω_c and the emitter frequency by ω_e . The index n refers to an individual cavity, and the index e refers to an individual emitter within a cavity. The operators for the creation and destruction of a photon in cavity n are given by a_n^\dagger and a_n respectively. The operators for the excitation and deexcitation of an emitter in cavity n are given by σ_n^+ and σ_n^- respectively. Such a system is shown in Fig. 1.

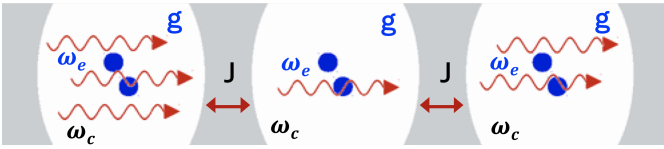


FIG. 1: A coupled-cavity array operating under the Tavis-Cummings-Hubbard model, with emitters represented by blue dots and photons represented by red arrows. J is the rate of photon hopping between cavities, g is the rate of cavity-emitter photon exchange, ω_c is the cavity frequency and ω_e is the emitter frequency. Figure adapted from Knap [12].

Experimentally, the parameter J is tuned by changing the separation between two adjacent photonic crystal cavities. This is accomplished by altering the number of nanoholes fabricated between the cavities, with fewer holes corresponding to a smaller separation and thus a larger J . This parameter is often expressed as $J/2\pi$, with typical values varying from a few GHz to a few hundred GHz [11].

The parameter g depends on how the emitter is positioned relative to the cavity’s electric field profile, as well as on the choice of color center. When expressed as $g/2\pi$, typical values are on the order of a few GHz [11].

In order to simplify our model, we do not consider losses to the environment. Loss processes, governed by the cavity energy decay rate κ and the emitter energy decay rate γ , are critical to take into account in any experimental realization. The addition of these terms to our computational model is feasible and is therefore an important area for further study.

The preliminary step in constructing the Hamiltonian given by Eq. 1 is to construct the basis of the system. This requires listing all possible states the system could be in. The overall system is described by the parameters N , M , and the number of emitters in each cavity. Given these parameters, the states describe the possible locations of the excitation(s). Consider, for example, a small system consisting of two cavities, one excitation, and a single emitter in the first cavity. This system has three possible states:

$$\begin{aligned} 1 |n_1\rangle 0 |n_2\rangle 0 |e_1\rangle & \text{— photon in first cavity} \\ 0 |n_1\rangle 1 |n_2\rangle 0 |e_1\rangle & \text{— photon in second cavity} \\ 0 |n_1\rangle 0 |n_2\rangle 1 |e_1\rangle & \text{— emitter in first cavity excited} \end{aligned}$$

where the $|n_i\rangle$ represent cavity sites and the $|e_i\rangle$ represent emitter sites. A coefficient of 1 indicates that there is an excitation in that site, and a coefficient of 0 indicates that there is no excitation.

The generation of all possible states by hand becomes tedious for systems with a greater number of excitations. This process was automated using a recursive algorithm. The algorithm is flexible, allowing the user to input any values for N and M and dictate the number of emitters in each cavity individually. We are limited only by the memory and runtime constraints on the diagonalization of our Hamiltonian.

The Hamiltonian gives a quantum mechanical description of the possible energy states of a system. In our case, construction of the Hamiltonian requires considering which states

in the basis are immediately accessible from a given current state. For example, each photon can hop either to the left or to the right to put the system into a new state. An emitter in the ground state can be excited by a photon in its cavity, and likewise an excited emitter can deexcite to create a photon in its cavity. Our algorithm systematically identifies each of these possible transitions for each state, and enters the corresponding terms into the Hamiltonian matrix. The basis states are stored in a hashtable data structure for efficient lookup. The user can set the individual values of J for each intercavity coupling, ω_c for each cavity, and ω_e and g for each emitter.

These two algorithms, for constructing the basis and constructing the Hamiltonian, together provide us with a flexible computational model to study the behavior of CCAs operating under the Tavis-Cummings-Hubbard model. The algorithms’ flexibility means that there is a large parameter space available for exploration. In this report, we focus on two different thrusts of investigation. The first is the use of defects to induce localization in a CCA. The second is quantum state transfer across a CCA.

A. Defects for Localization

Localization in a CCA is defined by the emergence of eigenstates in which the excitation(s) have a very large probability of existing in a small region of the array, and a low probability of existing elsewhere. These eigenstates are known as localized modes, whereas eigenstates with a more even probability distribution are known as extended modes. For both classical and quantum systems, it is well known that the introduction of a “defect” typically induces localization at the site of that defect [13]. For example, in a homogeneous coupled mass-spring chain, if we replace a single spring with a spring of larger spring constant, we will observe an eigenstate in which only the masses near the defect spring oscillate [14, 15].

In this report, we investigate the use of emitters to induce localization in a CCA operating under periodic boundary conditions. Specifically, we can introduce a defect cavity containing an emitter into an emitter-free CCA. This topic is easily studied with exact diagonalization, because localization effects can be observed directly from the eigenvalues and eigenvectors of the system. Thus, to generate our data, we simply diagonalize Eq. 1 numerically for a given set of parameters.

B. Quantum State Transfer

The question of how to transmit a quantum state across a network is a key issue in quantum information research. In a chain of coupled qubits, this means transferring an arbitrary quantum state of the qubit located at one end of the chain to the qubit at the other end. Many proposals have focused on implementations using spin chains, or arrays of spin-1/2 particles undergoing spin-spin interactions [16, 17]. CCAs have attracted interest because they can serve as experimental realizations of spin chains [4].

Quantum state transfer (QST) is a transmission mechanism in which we initialize a quantum state at one end of a spin chain and then simply let the system evolve in time until the state appears at the opposite end of the chain. This method is attractive because no outside control or manipulation of the system is required after the initialization [2].

Unfortunately, due to dispersion of the initial wavepacket, perfect state transfer is impossible for homogeneous spin chains with $N > 3$. Perfect transfer can be achieved, however, by engineering each intercavity coupling value J_n . One such scheme is shown in Fig. 2, where the J_n are engineered according to $J_n = \sqrt{n * (N - n)}$, where N is the chain length and n is the index of the current site [17].

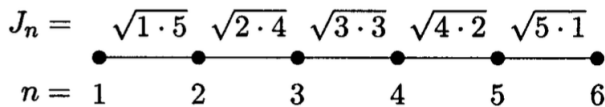


FIG. 2: A coupled-cavity array with six cavities where the intercavity coupling rates J_n are individually engineered to facilitate perfect quantum state transfer. In this case, the J_n are set by $J_n = \sqrt{n * (N - n)}$, where N is the chain length and n is the index of the current site. Figure from Christandl [17].

The need to individually engineer each J_n poses an experimental challenge. Because of this drawback, researchers have investigated proposals to achieve near-perfect QST by altering only the outermost coupling values [3, 18, 19]. This would allow the spin chain to remain largely homogeneous. Although most research in this area has dealt with generic spin chains, several papers have focused on CCA implementations specifically, including CCAs in which every cavity contains an emitter [2].

We are interested in investigating if “defects” in parameters other than J_n can facilitate robust state transfer. Specifically, we consider whether we can achieve robust QST by placing emitters in the outermost cavities, while the other cavities contain no emitters.

We investigate QST by looking at the time evolution of our system. We must calculate $|\psi(t)\rangle$ given the system’s initial state $|\psi(0)\rangle$. This is accomplished with the standard quantum mechanical formulation for time evolution:

$$|\psi(t)\rangle = U * |\psi(0)\rangle \quad (2)$$

$$U = e^{-iHt} = S e^{-iDt} S^T. \quad (3)$$

Here, H is the time-independent Hamiltonian, S is the matrix with the eigenvectors of H as its columns, and D is the diagonalized version of H . We take $\hbar = 1$.

QST from one end of a CCA to the other necessitates the use of open boundary conditions, as opposed to the periodic boundary conditions we assumed for the study of localization.

III. INDUCING LOCALIZATION WITH EMITTERS

We first look at a system with $N = 40$ cavities and one excitation. Periodic boundary conditions are implemented. None of the cavities contains an emitter. We choose $J = 1$, and set $\omega_c = 0$ for simplicity. Figure 3 depicts the expected eigenspectrum of this system, given by

$$E(n) = \omega_c - 2J \cos\left(\frac{2\pi n}{N}\right) \quad (4)$$

where n is an integer with $0 \leq n \leq N$. Equation 4 is derived by applying the tight-binding approximation, first introduced in condensed matter physics, to the coupled-cavity array [20]. Note the presence of degenerate eigenvalues in Fig. 3, which arise from the fact that

$$\cos\left(\frac{2\pi n}{N}\right) = \cos\left(\frac{2\pi(N - n)}{N}\right). \quad (5)$$

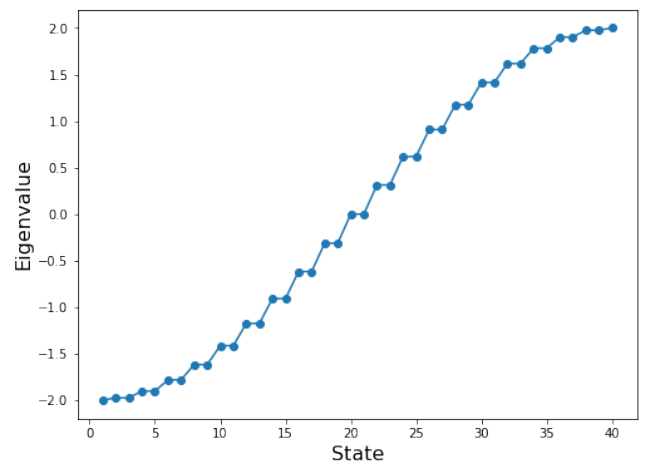


FIG. 3: The eigenspectrum of a coupled-cavity array system with 40 cavities, one excitation, and no emitters. We set the intercavity coupling rate $J = 1$ and the cavity frequency $\omega_c = 0$. The eigenvalues are displayed in ascending order from left to right, so the first eigenvalue corresponds to the lowest-energy state and the fortieth eigenvalue corresponds to the highest-energy state. The eigenspectrum is described by Eq. 4.

We proceed by adding one emitter in the twentieth cavity, while the other cavities still contain no emitters. The cavity choice is arbitrary due to the presence of periodic boundary conditions. We keep $J = 1$ and choose $g = 3$ such that excitation is preferred over hopping. We set $\omega_e = 0$ for simplicity. Figure 4 shows that this setup causes the emergence of one outlier eigenstate above the band and another outlier eigenstate below the band. The defect also causes the loss of degeneracy.

The squared components of the lowest-energy eigenvector are depicted in Fig. 5. It is clear that the excitation is very likely to be found the cavity containing the emitter, either as

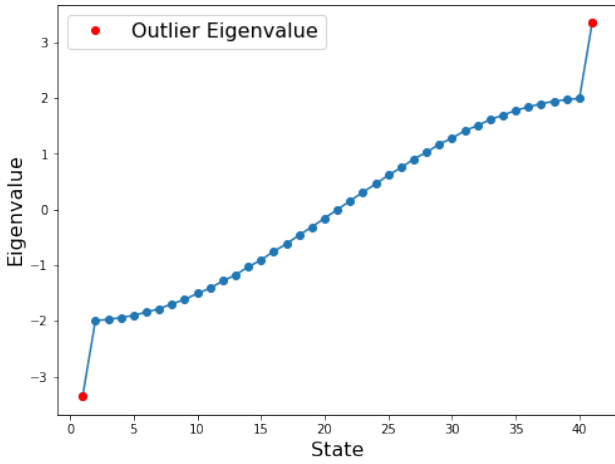


FIG. 4: The eigenspectrum of a coupled-cavity array system with 40 cavities, one excitation, and one emitter in the twentieth cavity. We set the intercavity coupling rate $J = 1$ and cavity-emitter photon exchange rate $g = 3$ such that excitation is preferred over hopping. Cavity frequency ω_c and emitter frequency ω_e are both set to zero for simplicity. The addition of an emitter in the twentieth cavity causes the emergence of one outlier eigenvalue above the band and another below the band.

a photon in that cavity or in the emitter itself. Thus, this is a localized state. The squared components of the highest-energy eigenvector are identical to those of the lowest-energy eigenvector, so this is a second localized state.

This analysis relies on the fact that $g > J$. If we instead set $g < J$ such that hopping is preferred over excitation, we no longer observe outlier eigenvalues below and above the band. We do, however, see two states that display some localization, with the excitation preferentially being found in the emitter. These two states fall in the middle of the band, corresponding to the twentieth and twenty-second eigenvectors. This suggests that when $g < J$, the two outlier eigenvalues migrate to the middle of the band.

We next examine how localization manifests itself when we introduce a block of cavities that each contain an emitter. We again consider our same system of 40 cavities with one excitation, with $J = 1$ and $g = 3$. Now, we add a single emitter to each of the five cavities in the center of the array (cavities 18-22). The location of the cavities is again arbitrary due to periodic boundary conditions. Figure 6 shows that we now observe five outlier eigenstates above the band and five below the band, corresponding to our block of five cavities. The photon is most likely to be found in the block of cavities with emitters, as can be seen in Fig. 7.

Overall, these results show that when we introduce emitters into one or several cavities of an emitter-free CCA, outlier states appear in the eigenspectrum if $g > J$. These correspond to modes in which the photon is localized at the cavity or cavities with emitters. When $g < J$, we observe modes that display localization at the emitter, but these states appear in the middle of the eigenspectrum rather than below and above the band.

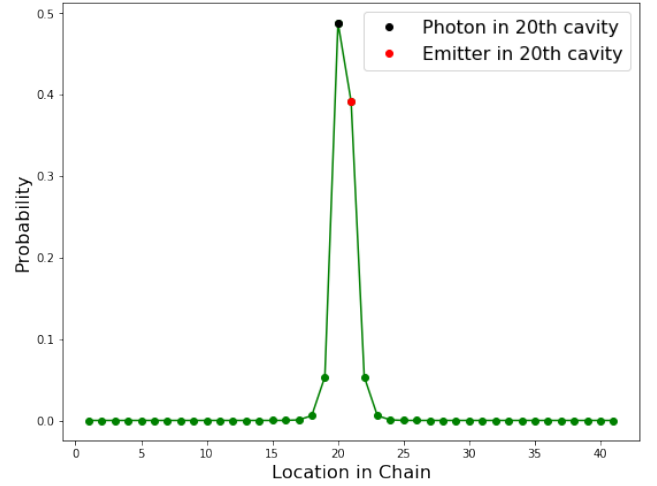


FIG. 5: The squared components of the lowest-energy eigenvector for a coupled-cavity array system with 40 cavities, one excitation, and one emitter in the twentieth cavity. The black dot represents the probability that the excitation will be found as a photon in the emitter's cavity. The red dot represents the probability that the excitation will be found in the emitter. The addition of the emitter causes this eigenvector to become a localized state, with the excitation most likely to be found in the cavity with the emitter.

IV. QUANTUM STATE TRANSFER WITH EMITTERS

Here we consider the possibility of achieving robust quantum state transfer across a CCA through the judicious placement of emitters. We show that for the correct parameters, a CCA with one emitter in each of the outermost cavities behaves identically to a CCA with the outermost J values modified and no emitters present. The latter is the system studied by Zwick *et. al* and Banchi *et. al.* for QST applications [18, 19].

In a CCA with an emitter in each edge cavity, we show that the two emitters effectively function as “pseudo-cavities.” An excitation in an emitter state has only the option to return to the ground state. In contrast, due to the presence of an emitter, an excitation in an edge cavity now has two options—to excite the emitter in that cavity or to hop to the adjacent cavity.

Thus, each emitter takes on the role of an outermost cavity, from which the excitation has only one option for movement. This means that a system of N cavities with one emitter in each edge cavity behaves similarly to a system of $N + 2$ cavities with no emitters (see Fig. 8). Note that this effect is present only when the emitters are placed in the outermost cavities. Placing an emitter in an interior cavity introduces a “branching” effect rather than increasing the effective length of the chain.

We now examine the conditions under which the two aforementioned systems behave identically. Consider a CCA of length N with uniform coupling strength J and cavity-emitter exchange rate g , with one emitter in each outermost cavity. Next, consider a CCA of length $N + 2$ with modified edge

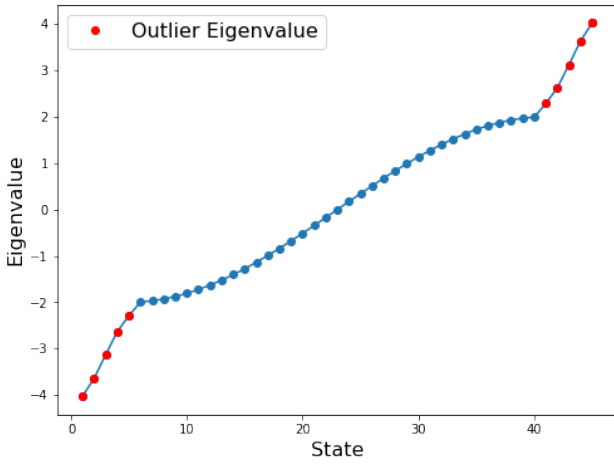


FIG. 6: The eigenspectrum of a coupled-cavity array system with 40 cavities, one excitation, and one emitter each in cavities 18-22. We set the intercavity coupling rate $J = 1$ and cavity-emitter photon exchange rate $g = 3$ such that excitation is preferred over hopping. Cavity frequency ω_c and emitter frequency ω_e are both set to zero for simplicity. The addition of the block of five emitters causes the emergence of five outlier eigenvalues above the band and five below the band.

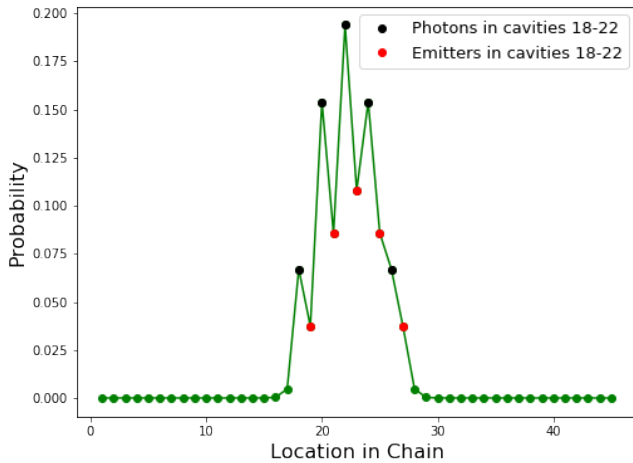


FIG. 7: The squared components of the lowest-energy eigenvector for a coupled-cavity array system with 40 cavities, one excitation, and one emitter each in cavities 18-22. The black dots represent the probabilities that the excitation will be found as a photon in a given emitter's cavity. The red dots represent the probabilities that the excitation will be found in a given emitter. The addition of the block of emitters causes the excitation to become localized within the block.

couplings J' and bulk coupling strength J_b , with no emitters present. The two CCAs will behave identically in the case that $J = J_b$ and $g = J'$. Under these conditions, their Hamiltonians are identical except that g and J' appear with opposite signs according to Eq. 1. The two Hamiltonians are in fact similar matrices and thus have identical eigenvalues. This

means that the time evolution of the two systems will be identical.

The placement of an emitter in each edge cavity could therefore serve as an alternative to detuned J values to facilitate significantly improved QST compared to a homogeneous CCA. This effect is demonstrated for an example system below.

We consider a CCA with 50 cavities, one excitation, and $J = 1$. We hope to transfer a quantum state across the array, from the first cavity to the fiftieth cavity, by initializing a state in the first cavity and then letting the system evolve in time.

Let us first consider this system with no emitters. We initialize the excitation in the first cavity. Figure 9 depicts the evolution of the system in time. We can see that the transfer is poor due to dispersion effects—that is, the state arrives at the fiftieth cavity with a probability of 41.6% percent, rather than 100 percent.

Next, we add a single emitter in the first and fiftieth cavities. We set $g = 0.554$ following Banchi's optimal J' value reported for an array with $N = 51$ cavities [19]. Banchi reports that this optimal value does not require fine-tuning, so the slight difference in N values can easily be neglected here. The excitation is initialized in the emitter state (rather than the photon state) of the first cavity. Figure 10 shows that the transfer fidelity improves greatly compared to the CCA with no emitters. The excitation appears in the emitter of the twenty-fourth cavity with a probability of 90.0 percent.

The system depicted in Fig. 10 behaves identically to a system with no emitters and with parameters $N = 52$, $J_b = 1$, and detuned edge couplings $J' = 0.554$, as was argued above. Thus, many of the conclusions of [18, 19] also apply to CCAs with one emitter in each end cavity. State transfer is poor in Fig. 9 due to dispersion of the initial wavepacket. In contrast, the system with emitters in its edge cavities experiences low dispersion and thus robust state transfer (see Fig. 10). Following Zwick and Banchi, this system operates in the ballistic regime, which is characterized by equally spaced eigenvalues in the middle of the band [18, 19]. The normal modes in this linear region of the eigenspectrum dominate the transmission dynamics. A system with all J_n engineered for perfect state transfer exhibits a perfectly linear eigenspectrum [17], while the edge detuning method approximates a linear spectrum without requiring the individual engineering of each cavity site.

The optimal J' value (corresponding to the optimal g value for the emitter system) is shown to scale as $N^{-1/6}$ for large N values [19]. Banchi reports that when using the optimal J' value, state transfer fidelity remains high even for very large N . The present report does not calculate fidelity values, which require averaging over all possible initial states $|\psi(0)\rangle$ from the Bloch sphere. The transmission probabilities reported here are for one particular $|\psi(0)\rangle$ corresponding to an excitation initialized in the first cavity.

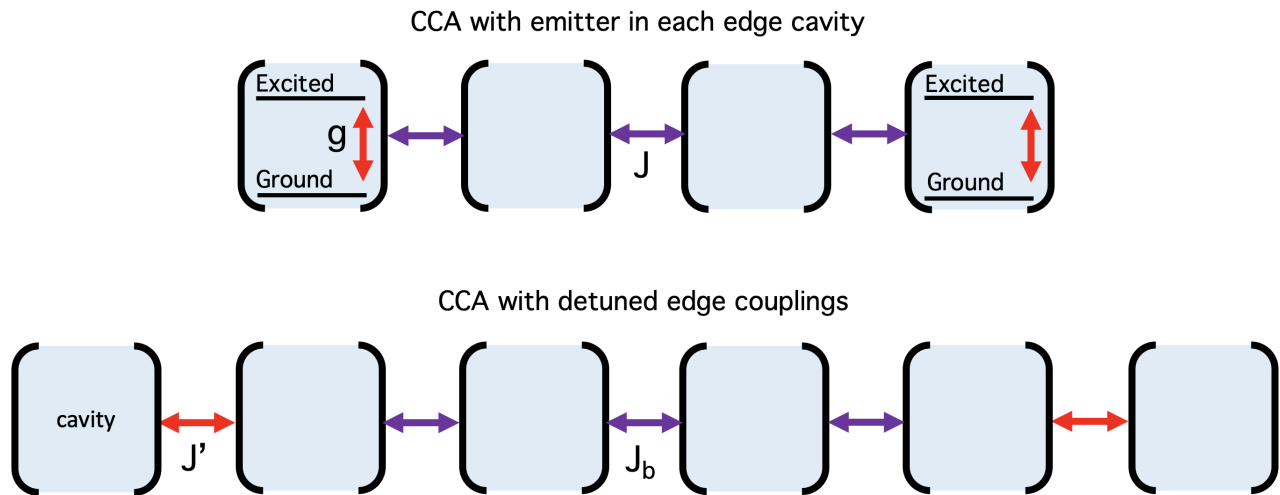


FIG. 8: Comparison of two coupled cavity arrays. The top array has $N = 4$ cavities and an emitter in each edge cavity. It has uniform intercavity coupling strength J and cavity-emitter exchange rate g . The bottom array has $N = 6$ cavities and bulk intercavity coupling strength J_b , with the edge couplings detuned to J' . The two systems will display identical time evolution if $J = J_b$ and $g = J'$. Each emitter's excited state functions as an additional “pseudocavity,” giving the two systems the same effective length.

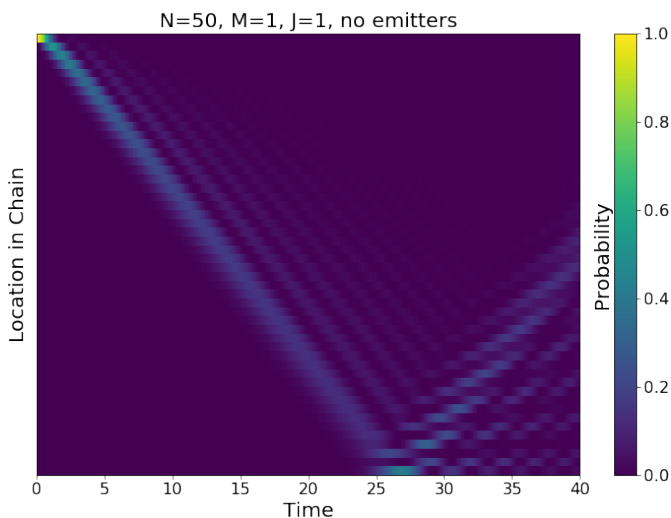


FIG. 9: Time evolution of a coupled cavity array system with $N = 50$ cavities, $M = 1$ excitation, and intercavity coupling strength $J = 1$. The system has no emitters. The excitation is initialized at one end of the array at time $t = 0$, and the system is then allowed to evolve in time without any interference. Transfer is poor, with the state having a 41.6% probability of arriving at the opposite end of the array at about $t = 26$.

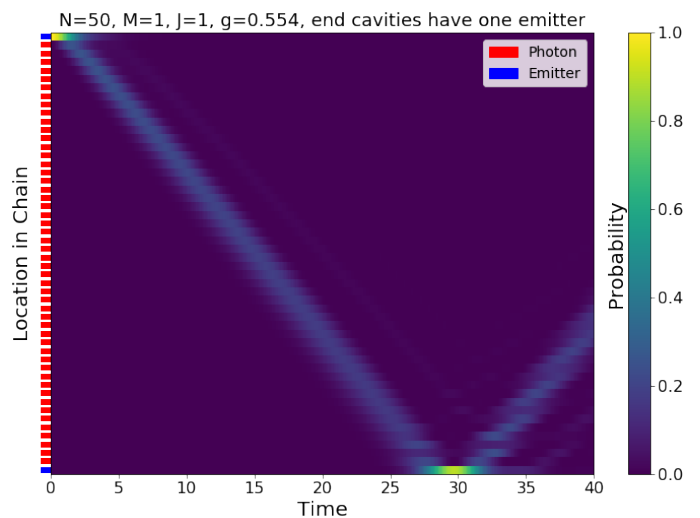


FIG. 10: Time evolution of a coupled cavity array system with $N = 50$ cavities, $M = 1$ excitation, intercavity coupling strength $J = 1$, and $g = 0.554$. The outermost cavity at each end of the array contains one emitter. The excitation is initialized in the emitter of the first cavity at time $t = 0$. Transfer is significantly improved compared to Fig. 9, with the excitation having a 90.0% probability of reaching the emitter in the fiftieth cavity at about $t = 29$.

V. CONCLUSIONS AND OUTLOOK

Coupled cavity arrays have attracted significant interest in recent years for their potential use in quantum many-body simulations and quantum information processing, as well as

the study of new regimes of light-matter interaction. Recent progress on the experimental side has been considerable, with CCA implementation now viable using photonic crystal resonators.

In this report, we use exact diagonalization to investigate CCAs operating under the Tavis-Cummings-Hubbard model.

We implement a computational model that performs exact diagonalization numerically, while permitting great flexibility in the system parameters. This model is used to study two separate aspects of CCA behavior, namely localization and quantum state transfer.

It is a familiar property that a “defect” in a system can be used to introduce localized modes at the site of the defect. We demonstrate that this effect occurs when an emitter is placed in one cavity of a CCA that otherwise contains no emitters. For an array with one excitation and $g > J$ (excitation preferred over hopping), the introduction of an emitter causes two outlier eigenstates to emerge, one below and one above the band. Similarly, when an emitter is added to each of n adjacent cavities, we see the emergence of n outlier eigenstates above the band and n below.

CCA systems are also a potential platform for quantum state transfer, in which a quantum state is initialized at one end of a spin chain and then allowed to evolve freely until it reaches the other end. For arrays with more than three cavities, perfect transfer can be achieved only by individually engineering each intercavity coupling strength J_n . To avoid this experimental difficulty, many proposals have focused on modifying only the outermost coupling values to facilitate robust state transfer in the ballistic regime.

We demonstrate the similarity between a system with modified edge couplings and a CCA with uniform J with an emitter placed in each outermost cavity. In particular, consider a CCA of length N with uniform intercavity coupling J , cavity-emitter exchange rate g , and one emitter in the first and last cavities. We show that this system is effectively equivalent to a CCA of length $N + 2$ with bulk coupling J_b , modified edge couplings J' , and no emitters present, in the case that $J = J_b$ and $g = J'$. Under these conditions, the Hamiltonians of the two systems are similar matrices and thus have identical eigenvalues, which means the systems have identical time evolution.

This result suggests that the placement of emitters in edge cavities could be used as an alternative to adjusting the outermost couplings as a means of facilitating robust QST. For a photonic crystal cavity implementation, this corresponds to fabricating a color center in each edge cavity rather than ad-

justing the number of nanoholes fabricated between the outermost adjacent cavities.

The QST results presented here could be furthered by calculating average fidelity values for the CCA with emitters in its edge cavities. This report presents only the probability of transfer for one specific case, that in which an excitation is initialized in the first cavity.

The connection between modified J values and the placement of emitters could also be investigated for other CCA arrangements. For example, [3] looks at adjusting the *two* outermost J values at each end of the array. In addition, [2] considers using a CCA with an emitter in each cavity to implement very weak outer J values, which facilitate QST with Rabi-like dynamics rather than in the ballistic regime. These dynamics involve the formation of localized modes at the array edges, so the conclusions of Section III may be relevant.

The Tavis-Cummings-Hubbard model, in contrast to the more standard Jaynes-Cummings-Hubbard model, permits the placement of multiple emitters in a single cavity of a CCA, a relatively new experimental possibility that is not considered in this report [10]. Thus, the results presented here could be reexamined for cases in which multiple emitters couple to a single cavity mode.

Lastly, our computational model does not account for loss processes. These parameters could be introduced to the model to more accurately simulate experimental dynamics.

VI. ACKNOWLEDGEMENTS

I would like to thank my mentors from the summer of 2020, Dr. Richard Scalettar and Dr. Marina Radulaski. Many thanks to Jesse Patton and other Radulaski group members for their advice and support, and to Dr. Rena Zieve and Dr. John Mahoney for their leadership and teaching within the UC Davis REU program. Finally, I would like to acknowledge the National Science Foundation for funding, and my undergraduate institution, Carleton College, for supporting me in applying for this REU opportunity.

-
- [1] M. J. Hartmann, F. G. S. L. Brandao, and M. B. Plenio, “Quantum many-body phenomena in coupled cavity arrays,” *Laser Photonics Rev.* **2**, 6, pp. 527-556 (2008).
 - [2] G. M. A. Almeida, F. Ciccarello, T. J. G. Apollaro, and A. M. C. Souza, “Quantum-state transfer in staggered coupled-cavity arrays,” *Phys. Rev. A* **93**, 032310 (2016).
 - [3] T. J. G. Apollaro, L. Banchi, A. Cuccoli, R. Vaia, and P. Verrucchi, “99%-fidelity ballistic quantum-state transfer through long uniform channels,” *Phys. Rev. A* **85**, 052319 (2012).
 - [4] M. J. Hartmann, F. G. S. L. Brandao, and M. B. Plenio, “Effective spin systems in coupled microcavities,” *Phys. Rev. Lett.* **99**, 160501 (2007).
 - [5] M. J. Hartmann, F. G. S. L. Brandao, and M. B. Plenio, “Strongly interacting polaritons in coupled arrays of cavities,” *Nature Physics* **2**, 12, pp. 849-855 (2006).
 - [6] D. G. Angelakis, M. F. Santos, and S. Bose, “Photon-blockade-induced Mott transitions and XY spin models in coupled cavity arrays,” *Phys. Rev. A* **76**, 031805 (2007).
 - [7] A. Tomadin and R. Fazio, “Many-body phenomena in QED-cavity arrays,” *J. Opt. Soc. Am B* **27**, 6, pp. 130-136 (2010).
 - [8] A. Majumdar, A. Rundquist, M. Bajcsy, V. D. Dasika, S. R. Bank, and J. Vuckovic, “Design and analysis of photonic crystal coupled cavity arrays for quantum simulation,” *Phys. Rev. B* **86**, 195312 (2012).
 - [9] M. J. Hartmann, “Quantum simulation with interacting photons,” *J. Opt.* **18**, 104005 (2016).
 - [10] M. Radulaski, “Silicon carbide and color center quantum photonics,” PhD thesis, Stanford University, 2017.
 - [11] S. Majety, V. A. Norman, L. Li, M. Bell, P. Saha, and M. Radulaski, “Quantum photonics in triangular-cross-section nanode-

- vices in silicon carbide,” <https://arxiv.org/pdf/2012.02350.pdf> (2020).
- [12] M. Knap, E. Arrigoni, and W. von der Linden, “Spectral properties of coupled cavity arrays in one dimension,” *Phys. Rev. B* **81**, 104303 (2010).
- [13] E. W. Montroll and R. B. Potts, “Effects of defects on lattice vibrations,” *Phys. Rev.* **100**, 2, pp. 525-543 (1955).
- [14] A. Aghamohammadi, M. E. Foulaadvand, M. H. Yaghoubi, and A. H. Mousavi, “Normal modes of a defected linear system of beaded springs,” *Am. J. Phys.* **85**, 3, pp. 193-201 (2017).
- [15] A. Kolan, B. Cipra, and B. Titus, “Exploring localization in nonperiodic systems,” *Comput. Phys.* **9**, 4, pp. 387-395 (1995).
- [16] S. Bose, “Quantum communication through an unmodulated spin chain,” *Phys. Rev. Lett.* **91**, 207901 (2003).
- [17] M. Christandl, N. Datta, A. Ekert, and A. J. Landahl, “Perfect state transfer in quantum spin networks,” *Phys. Rev. Lett.* **92**, 187902 (2004).
- [18] A. Zwick, G. A. Álvarez, J. Stolze, and O. Osenda, “Spin chains for robust state transfer: modified boundary couplings versus completely engineered chains,” *Phys. Rev. A* **85**, 012318 (2012).
- [19] L. Banchi, T. J. G. Apollaro, A. Cuccoli, R. Vaia, and P. Verucchi, “Long quantum channels for high-quality entanglement transfer,” *New. J. Phys.* **13**, 123006 (2011).
- [20] M. Notomi, E. Kuramochi, and T. Tanabe, “Large-scale arrays of ultrahigh-Q coupled nanocavities,” *Nat. Photonics* **2**, 096501 (2008).